



Regional brain network organization distinguishes the combined and inattentive subtypes of Attention Deficit Hyperactivity Disorder



Jacqueline F. Saad^{a,b}, Kristi R. Griffiths^a, Michael R. Kohn^{a,c}, Simon Clarke^{a,c},
Leanne M. Williams^{d,e}, Mayuresh S. Korgaonkar^{a,b,*}

^a Brain Dynamics Centre, The Westmead Institute for Medical Research, The University of Sydney, Australia

^b The Discipline of Psychiatry, University of Sydney Medical School: Western, Westmead Hospital, Australia

^c Centre for Research into Adolescents' Health, Department of Adolescent and Young Adult Medicine, Westmead Hospital, Australia

^d Psychiatry and Behavioral Sciences, Stanford University, Stanford, CA, USA

^e MIRECC, Palo Alto VA, Palo Alto, CA, USA

ARTICLE INFO

Keywords:

ADHD
Predominantly inattentive type
Combined type
Structural connectome
Volume
Graph theory

ABSTRACT

Attention Deficit Hyperactivity Disorder (ADHD) is characterized clinically by hyperactive/impulsive and/or inattentive symptoms which determine diagnostic subtypes as Predominantly Hyperactive-Impulsive (ADHD-HI), Predominantly Inattentive (ADHD-I), and Combined (ADHD-C). Neuroanatomically though we do not yet know if these clinical subtypes reflect distinct aberrations in underlying brain organization.

We imaged 34 ADHD participants defined using DSM-IV criteria as ADHD-I ($n = 16$) or as ADHD-C ($n = 18$) and 28 matched typically developing controls, aged 8–17 years, using high-resolution T1 MRI. To quantify neuroanatomical organization we used graph theoretical analysis to assess properties of structural covariance between ADHD subtypes and controls (global network measures: path length, clustering coefficient, and regional network measures: nodal degree). As a context for interpreting network organization differences, we also quantified gray matter volume using voxel-based morphometry.

Each ADHD subtype was distinguished by a different organizational profile of the degree to which specific regions were anatomically connected with other regions (i.e., in “nodal degree”). For ADHD-I (compared to both ADHD-C and controls) the nodal degree was higher in the hippocampus. ADHD-I also had a higher nodal degree in the supramarginal gyrus, calcarine sulcus, and superior occipital cortex compared to ADHD-C and in the amygdala compared to controls. By contrast, the nodal degree was higher in the cerebellum for ADHD-C compared to ADHD-I and in the anterior cingulate, middle frontal gyrus and putamen compared to controls. ADHD-C also had reduced nodal degree in the rolandic operculum and middle temporal pole compared to controls. These regional profiles were observed in the context of no differences in gray matter volume or global network organization.

Our results suggest that the clinical distinction between the Inattentive and Combined subtypes of ADHD may also be reflected in distinct aberrations in underlying brain organization.

1. Introduction

Attention Deficit Hyperactivity Disorder (ADHD) is a common heterogeneous neurodevelopmental condition affecting approximately 5% of children and 2.5% of the adult population (Faraone et al., 2015) and is characterized by the onset of pervasive behavioral symptoms prior to age twelve years, affecting academic, occupational and social

functioning. Clinical symptoms are categorized as (i) inattentive and/or (ii) hyperactive/impulsive to determine three diagnostic subtypes (i.e. presentations in DSM-V): predominantly inattentive (ADHD-I), predominantly hyperactive-impulsive (ADHD-HI), or combined: inattentive and hyperactive-impulsive (ADHD-C) (Association, A.P., 2013) with the ADHD-I & ADHD-C reported as the most common types presented clinically (Willcutt, 2012).

Abbreviations: ACC, anterior cingulate cortex; ADHD, Attention Deficit Hyperactivity Disorder; ADHD-I, predominantly inattentive presentation; ADHD-C, combined presentation; ADHD-HI, predominantly hyperactive-impulsive; ADHD-RS-IV, Attention Deficit/Hyperactivity Disorder Rating Scale; CPRS-LV, Conners' Parent Rating Scale-Revised: Long Version; DSM-V, Diagnostic Manual of Statistical Disorders fifth edition; DICA, Diagnostic Interview for Children and Adolescents; DMN, default mode network; GM, gray matter; iSPOT-A, international study to predict optimized treatment in ADHD; MINI Kid, Mini International Neuropsychiatric Interview; MPH, methylphenidate

* Corresponding author at: Brain Dynamics Centre, The Westmead Institute for Medical Research, 176 Hawkesbury Road, Westmead, NSW 2145, Australia.

E-mail address: m.korgaonkar@sydney.edu.au (M.S. Korgaonkar).

<http://dx.doi.org/10.1016/j.nicl.2017.05.016>

Received 28 October 2016; Received in revised form 10 April 2017; Accepted 21 May 2017

Available online 22 May 2017

2213-1582/© 2017 The Authors. Published by Elsevier Inc. This is an open access article under the CC BY-NC-ND license (<http://creativecommons.org/licenses/by-nc-nd/4.0/>).

Measures of clinical symptoms routinely utilized are subjective, with little understanding of the underlying pathophysiology of each of these ADHD subtypes (Bush, 2010). The emergence of neuroimaging studies over the last three decades has provided opportunities to complement clinical and behavioral measures in advancing the ADHD neurobiological framework (Saad et al., 2015; Valera et al., 2007). Recent reviews of neuroimaging studies investigating brain function and structural volumetric abnormalities in children/adolescents with ADHD highlight both functional and structural alterations in regions such as the prefrontal, frontal and cerebellar cortices, anterior cingulate cortex (ACC), ventral striatum and the basal ganglia (Nakao et al., 2011; Seidman et al., 2005; Cortese et al., 2012). However, these studies often utilize a pooled ADHD population sample without reference to ADHD subtypes and may be prone to confounding bias due to known heterogeneity among ADHD subtypes (Seidman et al., 2005). Consequently, it remains unclear whether the neurobiological mechanisms underlying the ADHD subtypes differ as variations of the condition or whether they may be distinct conditions. In this study, we investigate whether differences in brain structural and network organization distinguish the two most common ADHD subtypes, predominantly inattentive (ADHD-I) and combined (ADHD-C).

Few neuroimaging studies have investigated the neurobiological differences between the ADHD subtypes and findings thus far have been equivocal (Fair et al., 2012a). Some structural imaging studies have found no significant volumetric differences globally or for specific sub-regions of the basal ganglia structures between the ADHD-I and ADHD-C subtypes (Pineda et al., 2002; Vilgis et al., 2016) and also relative to controls (Wellington et al., 2006). Conversely, bilaterally smaller volumes of the caudate and ACC have been reported in ADHD-C children, relative to both ADHD-I type and controls, though the ADHD-I type did not differ from controls in this study (Semrud-Clikeman et al., 2014). In contrast, another study found reduced volume of the left medial frontal gyri, ACC, caudate and thalamus and right postcentral gyrus gray matter in the ADHD-I type relative to controls (de Mello et al., 2013). Further, smaller global gray matter volumes in the frontal, parietal, temporal and occipital lobes were observed in children with ADHD-C relative to controls (Batty et al., 2010). While findings of structural differences between ADHD subtypes are limited, there is further support for different neurobiological mechanisms underlying these subtypes from functional neuroimaging studies. Task-based fMRI studies have indicated frontoparietal and motor deficits in the ADHD-I type relative to both controls (Orinstein & Stevens, 2014) and ADHD-C type (Solanto et al., 2009). Additionally, dysfunction of regions associated with attentional cortical networks in the ADHD-C type relative to controls has been found (Silk et al., 2005; Stevens et al., 2007).

More recently neuroimaging and ADHD research have been geared toward the integration of connectivity measures; indicative of a paradigm shift from brain regional abnormalities to the role of *inter-regional* network dysfunction (Cao et al., 2014). This direction indeed provides a more holistic picture of the underlying neurobiology. Growing evidence from both functional and structural connectivity studies highlight brain connectivity differences in ADHD and between subtypes, which extends support for specific key networks that may underlie the combined and inattentive types (Carmona et al., 2015; Park et al., 2016; Iannaccone et al., 2015; Wang & Li, 2015). Correspondingly, diffusion tensor imaging (DTI) studies provide further support for distinct structural and white matter connectivity disturbances between the ADHD-C and ADHD-I subtype (Hong et al., 2014; Lei et al., 2014a; Svatkova et al., 2016; Ercan et al., 2016). A novel connectivity approach which complements both DTI and functional connectivity is connectivity mapping using the covariance of brain regional volumes (Singh et al., 2013; Griffiths et al., 2016). The integration of structural regional brain abnormalities using gray matter volume and structural network connectivity properties to measure structural covariance of brain regions (Alexander-Bloch et al., 2013)

may provide novel insights toward phenotypic differences that underlie the ADHD-I and ADHD-C presentations. Structurally and functionally connected brain regions tend to exhibit coordinated fluctuations in gray matter volume over time due to mutually trophic influences (Alexander-Bloch et al., 2013) and evaluating their network level properties using graph analysis may be critical to evaluate anatomical disorganization especially in ADHD in which cortical maturational delay is one of the leading etiological theories (Shaw et al., 2007) and other known network abnormalities (Bush, 2010). Further, differential rates of maturation in networks underlying inattentive and hyperactive/impulsive symptoms may explain the diminishing symptoms of hyperactivity/impulsivity over time in contrast to the relatively stable inattentive symptoms observed between the subtypes (Lee et al., 2016).

Global brain network topology may be derived using graph analysis measures of global and local efficiency, characteristic path lengths and clustering coefficient to assess brain network integration (Lei et al., 2014b). This study used measures of characteristic path length and clustering coefficient. The characteristic path length measures the number of connections between nodes which transfer information, while the clustering coefficient measures the connectedness of nodes within a network and their efficiency at relaying information (He & Evans, 2010). This approach is therefore well suited to tease out developmental related neurobiological connectivity differences underlying these symptoms and may provide novel insights toward network phenotypic differences that underlie the ADHD subtypes.

One key brain network consistently highlighted as atypical in ADHD across task-based (Peterson et al., 2009; Liddle et al., 2011) and resting-state (Carmona et al., 2015; Barber et al., 2015; Dey et al., 2012; Fair et al., 2010; Sripada et al., 2014; Tomasi & Volkow, 2012) fMRI, and structural volumetric (Carmona et al., 2005) studies is the default mode network (DMN). The DMN acts as a state regulation mechanism during task performance bearing implications for goal-directed activity, motivational effort and attention dysregulation in ADHD (Metin et al., 2015). Typically, the DMN exhibits increased activity during rest states (i.e. internalized ruminative thinking) and is suppressed in response to increased external cognitive demand (Raichle, 2015). Therefore, impaired modulation of the DMN to downregulate during task subsequent to compromised sustained attention is associated with increased task errors and diminishing attentional performance (Posner et al., 2014; Weissman et al., 2006) and may explain symptoms of impulsivity and impaired response inhibition associated with ADHD-C type (Fair et al., 2012a; Lin et al., 2015; Mohan et al., 2016). This is supported by functional connectivity studies that have examined both the ADHD-I and ADHD-C subtypes relative to controls (Fassbender et al., 2009; Liddle et al., 2011). A very small number of studies specifically report that this network may be disorganized between the subtypes of ADHD. A recent study used classification analysis of multi-modal imaging and phenotypic data and found structural graph theory network measures of the DMN to be associated with the ADHD-I type relative to ADHD-C type, ADHD-HI type, and controls (Anderson et al., 2014). Resting-state functional connectivity MRI (rs-fcMRI) studies incorporating graph theoretical analysis have observed distinct neural differences in the sensorimotor and default mode network (DMN) in the ADHD-C type relative to ADHD-I type (Fair et al., 2012a; dos Santos Siqueira et al., 2014) and ADHD-I type relative to controls (Qiu et al., 2011). Whether these functional differences in the DMN are also reflected in volume and structural covariance within this network is yet to be established.

This study used T1 magnetic resonance imaging (MRI) scans to investigate whether brain structural network organization may characterize the ADHD-I and ADHD-C subtypes relative to each other and neurotypical controls. We used both voxel-based morphometry analysis (VBM) and graph theory network analysis of whole brain inter-regional structural covariance networks to first investigate global and regional network level characteristics underlying these two ADHD subtypes. We also quantified volume as a context to investigate the network differences and also for overall volumetric characteristics underlying

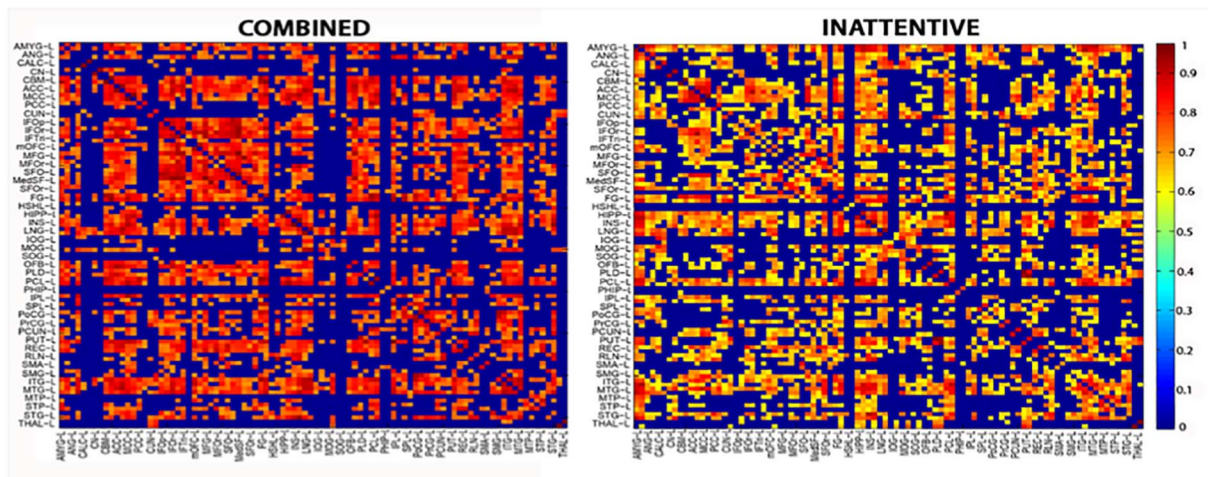


Fig. 1. T1 images were parcellated into 92 cortical and subcortical gray matter regions defined using the AAL atlas to create structural covariance networks in each group.

these subtypes. Additionally, based on the emerging evidence in the literature regarding atypical DMN connectivity in ADHD and functional evidence of differences within this network between the two types, we assessed structural volumetric and network characteristics of the DMN in both the ADHD-I and ADHD-C subtypes.

2. Methods and materials

2.1. Participant characteristics and study procedure

Participants were recruited as part of the International Study to Predict Optimized Treatment in ADHD (iSPOT-A) study. A detailed account of the inclusion/exclusion criteria protocols for participant recruitment, diagnostic measures, and procedures for the iSPOT-A study has been previously published (Elliott et al., 2014). Magnetic resonance imaging (MRI) data collected at Westmead Hospital, Sydney as part of the baseline data collection for the iSPOT-A study were available for 34 participants with ADHD (mean = 13.28; \pm 2.75; range 8–17 years) and 28 age and gender-matched typically developing controls (mean = 13.09; \pm 2.63; range 8–17 years). Confirmation of ADHD diagnosis (DSM-IV criteria), subtype (i.e. presentation in DSM-V) and severity was measured by the Mini International Neuropsychiatric Interview (MINI Kid) (Sheehan et al., 1998), the Attention Deficit/Hyperactivity Disorder Rating Scale (ADHD-RS-IV) (DuPaul, 1998) and symptom severity assessed using the ADHD-RS-IV scores (requires a score of > 1 on 6 or more subscale items on the Inattentive and/or Hyperactive/Impulsive subscales) and the Conners' Parent Rating Scale-Revised: Long Version (CPRS-LV) (Elliott et al., 2014). Of the 34 ADHD participants, 16 met diagnostic criteria for ADHD-C type (mean = 12.81 \pm 2.85; 4 females), while 18 met diagnostic criteria for the ADHD-I type (mean = 13.70 \pm 2.67; 5 females). Seven ADHD-C participants and three ADHD-I participants were diagnosed with comorbid oppositional defiant disorder. All ADHD participants were medication-free at the time of testing; 21 were medication naïve; 13 were treatment experienced with methylphenidate and were withdrawn from methylphenidate for at least 5 half-lives. Participants were all fluent in English and had no history of brain injury, any significant medical condition affecting brain function (e.g. epilepsy), or any contraindications for MRI. All participants and/or their guardians provided written informed consent to participate in the research, in accordance with National Health and Medical Research council guidelines.

2.2. Image acquisition and preprocessing

Magnetic resonance images were acquired using a 3.0 T GE Signa

HDx scanner (GE Healthcare, Milwaukee, Wisconsin) using an 8-channel head coil. Three-dimensional (3-D) T1-weighted magnetic resonance images were acquired in the sagittal plane using a 3D SPGR sequence (TR = 8.3 ms; TE = 3.2 ms; flip Angle = 11°; TI = 500 ms; NEX = 1; ASSET = 1.5; Frequency direction: S/I). A total of 180 contiguous 1 mm slices were acquired with a 256 \times 256 matrix, with an in-plane resolution of 1 mm \times 1 mm resulting in isotropic voxels. Pre-processing of the T1-weighted images was performed using the VBM8 toolbox (<http://dbm.neuro.uni-jena.de>), implemented within the SPM8 package (<http://www.fil.ion.ucl.ac.uk/spm>). First, MRI datasets were visually inspected for artifacts and movement, and all scans passed an automated quality assurance protocol within VBM8. Images were corrected for bias field inhomogeneity and tissue-classified into gray matter, white matter and cerebrospinal fluid. Study-specific (child/adolescent) tissue probability maps were created using the template-o-matic toolbox (Wilke et al., 2008) and implemented during registration to standard space using high dimensional DARTEL normalization. Warped tissue type images were modulated to preserve the volume of a particular tissue within a voxel by multiplying voxel values in the segmented images by the Jacobian determinants derived from spatial normalization. This allows for analysis of regional differences in absolute volume of tissue class.

2.3. Structural covariance network analysis

Individual, modulated, normalized non-linear GM images were parcellated into 92 cortical and subcortical gray matter regions defined using the AAL atlas to create structural covariance networks (92 \times 92 association matrix) in each group (Fig. 1). Using the WFU PickAtlas Toolbox (Maldjian et al., 2003), we generated 92 cortical and subcortical regions including the cerebellum. The cerebellum was generated by combining the eighteen cerebellar sub-regions (vermis not included due to lack of lateralization). Using a 92 \times 92 association matrix, R , was generated to create a structural covariance network for each group. Each entry, r_{ij} , was defined as the Pearson correlation coefficient between gray matter volume measures of regions i and j , across participants (He et al., 2007; Hosseini et al., 2012). A binary, undirected adjacency matrix was derived from each association matrix, whereby each coefficient was considered 1 if it was greater than a specific threshold and zero otherwise. The diagonal elements of the association matrix represent self-connections and were therefore excluded from analysis.

2.4. Graph theoretical analysis

Graph theoretical analyses were performed on these interregional

connectivity matrices using the Brain Connectivity Toolbox (<http://www.brain-connectivity-toolbox.net/>) (Rubinov & Sporns, 2010) and the Graph Analysis Toolbox (Hosseini et al., 2012).

2.4.1. Global network analysis

To allow a comparison of network properties between groups and avoid biases associated with using a single threshold, the association matrices were thresholded at a range of network densities in 0.01 steps (Dmin:0.01:0.50). The minimum density is that at which the networks of both groups were not fragmented and paths exist between each node and every other node. The maximum density chosen was 0.50, as after this threshold the graphs become increasingly random (Hosseini et al., 2012). At each of these thresholds, we calculated the following global network measures: 1) the characteristic path length (the mean number of connections on the shortest path between any two regions in the network and is a measure of network integration); and 2) the clustering coefficient (quantification of the probability that two nodes connected to an index node are also connected to each other and is a representation of network segregation). Evaluation of these topological measures was benchmarked against corresponding mean values of a null random graph. We generated null networks from covariance matrices that were matched to the distributional properties of the observed covariance matrix using the Hirschberger-Qi-Steuer algorithm (Hirschberger et al., 2007). As network metrics were calculated across each of the specified densities (Dmin: 0.02:0.50), they were represented by a curve depicting the change in network metric as a function of network density. Functional data analysis (FDA) was used to examine group differences in these curves across the global and DMN network measures as a function ($y = f(x)$) (Singh et al., 2013). This approach compares the two groups by summation of the curves in y values across a range of densities to avoid biases using a single threshold (Hosseini et al., 2012). Permutation tests as described below were applied to the FDA results to determine if there were significant group differences (Nichols & Hayasaka, 2003).

To evaluate network-level properties for the DMN, we created a structural covariance network utilizing regions associated with the DMN (described below). Only global properties for the DMN were evaluated, as described above.

2.4.2. Regional network analysis

Local nodal characteristics of individual network regions were also examined using the nodal degree, which is the number of connections that a node has with the rest of the network. Nodes were normalized by the mean network degree of each group prior to between-group comparisons (Singh et al., 2013).

2.4.3. Comparison between groups

A nonparametric permutation test with 1000 repetitions was conducted to test the statistical significance of both the global and regional network topologies. In every permutation, each participant was randomly reassigned to the ADHD subtype or control groups such that each group maintained their original number of subjects. We subsequently obtained an association matrix for each randomized group, thresholded at a range of network densities, which led to a binary adjacency matrix at each threshold. Network measures were calculated for all binary adjacency matrices at each density. Differences in network measures between randomized groups were then calculated, resulting in a permutation distribution of difference under the null hypothesis. Differences in ADHD subtype and control network measures were placed in the corresponding permutation distribution and 2-tailed *p*-values were calculated based on their position (Bernhardt et al., 2011). We report at a *p* level of 0.05 false discovery rate (fdr) corrected for regional network differences (Nichols & Hayasaka, 2003). The fdr corrections were used to correct for multiple comparisons across measures and regions. For the global network analyses, they were used to control for the assessment of 2 different metrics (characteristic path

length and clustering coefficient). For the regional network measures, fdr was used to account for comparisons across 92 regions.

2.5. Voxel-based morphometry analysis

We assessed volumetric differences between the ADHD-C and ADHD-I subtypes in addition to controls using voxel-wise two sample *t*-tests corrected for multiple comparisons (family wise error). Firstly, whole brain analyses were conducted using individual modulated, normalized non-linear GM images (i.e. corrected for total brain volume) using a statistical threshold of $p < 0.05$ corrected. Secondly, for the DMN region of interest (ROI) analyses, we combined thirteen ROI's identified in a previous study to create a single ROI mask for the DMN region (Fair et al., 2008). The regions of interest in the default mode network comprised the ventromedial prefrontal cortex, anterior medial prefrontal cortex posterior cingulate cortex, and the bilateral superior frontal cortex, lateral parietal cortex, inferior temporal cortex, parahippocampal gyrus, cerebellar tonsils and retrosplenial cortex (Fair et al., 2008). Regional ROI masks were created using an 8 mm sphere on MNI coordinates. We also evaluated volumetric differences for the regions which showed significant differences in nodal degree.

3. Results

Demographic and clinical characteristics of participants with ADHD-C type, ADHD-I type, and controls are summarized in Table 1. No significant differences were present between the two subtypes or relative to controls in terms of age and gender ratio. The two subtypes did not significantly differ on medication treatment history or ADHD-RS-IV (inattentive symptom items) the sum of items 1–9. However, as expected, ADHD-C type significantly differed from ADHD-I on the sum of items 10–18 (hyperactive/impulsive symptom items) and total item scores on the ADHD-RS-IV, respective of combined type criteria and severity. All of the ADHD-I type participants qualified for less than four out of 9 hyperactive/impulsive subscale items: 4 items ($n = 4$), 3 items ($n = 2$), 2 items ($n = 1$) and ≤ 1 item ($n = 11$). Whereas 15 out of 16 ADHD-C type participants qualified for six or more hyperactive/impulsive subscale items. These ADHD-RS-IV item counts have been summarized in Table S1 and S2 in the Supplementary material.

3.1. Structural covariance network analysis

3.1.1. Global network measures

Confirmed by FDA analysis, no global network differences were found in path length or normalized clustering between the two subtypes ($p > 0.05$) or relative to controls (Table 2).

Table 1
Participant demographic and clinical characteristics.

| | ADHD combined ($n = 16$) Mean \pm SD | ADHD Inattentive ($n = 18$) Mean \pm SD | Controls ($n = 28$) Mean \pm SD |
|--------------------------------|--|---|---|
| Gender, female <i>n</i> (%) | 4 (25%) | 5 (28%) | 9 (32%) |
| Age, years | 12.81 \pm 2.85 | 13.70 \pm 2.67 | 13.09 \pm 2.63 |
| ADHD-RS-IV sum items 1–9 | 20.94 \pm 3.55 | 21.61 \pm 3.66 | – |
| ADHD-RS-IV sum items 10–18 | 19.00 \pm 3.16 ^a | 7.89 \pm 4.04 | – |
| ADHD-RS-IV Total Item score | 39.94 \pm 5.05 ^a | 29.50 \pm 5.35 | – |
| Medication Naïve | 8 (50%) | 13 (72%) | – |
| Comorbidity, ODD | 7 (44%) | 3 (17%) | – |

Note: ADHD-RS-IV, Attention Deficit Hyperactivity Disorder rating scales- version 4; ODD, oppositional defiant disorder.

^a $p < 0.05$ for comparisons between the ADHD Combined and ADHD Inattentive subtype.

Table 2
Global network measures and regional nodal degree differences between the combined and inattentive ADHD subtypes.

| | ADHD combined (n = 16) | ADHD inattentive (n = 18) | Corrected p value |
|-----------------------------------|---------------------------|------------------------------|----------------------|
| Global network measures | Mean ± SD | Mean ± SD | |
| Normalized clustering coefficient | 0.95 ± 0.01 | 0.96 ± 0.01 | NS |
| Path length | 0.84 ± 0.02 | 0.96 ± 0.01 | NS |
| Regional nodal degree | | | |
| Calcarine_L | 0.225 | 1.199 | 0.032 |
| Hippocampus_L | 0.699 | 1.674 | 0.040 |
| Occipital_Sup_R | 0.100 | 1.199 | 0.025 |
| SupraMarginal_R | 0.824 | 1.499 | 0.045 |
| Cerebellum_L | 1.498 | 0.650 | 0.024 |

3.1.2. Regional network measures

Group comparison of regional network measures revealed ADHD-I type had greater nodal degree than ADHD-C type in the left calcarine ($p_{FDR} = 0.032$), left hippocampus ($p_{FDR} = 0.024$), the right superior occipital ($p_{FDR} = 0.025$), and the right supramarginal gyrus ($p_{FDR} = 0.045$). ADHD-C type exhibited greater nodal degree than ADHD-I type in the left cerebellum ($p_{FDR} = 0.024$) (Fig. 2). ADHD-I type, comparatively to controls, exhibited greater nodal degree in the bilateral amygdala (left, $p_{FDR} = 0.017$, right, $p_{FDR} = 0.047$) and bilateral hippocampus (left, $p_{FDR} = 0.004$, right, $p_{FDR} = 0.014$). Relative to controls, ADHD-C type exhibited greater nodal degree in the left anterior cingulum ($p_{FDR} = 0.045$), left middle frontal gyrus ($p_{FDR} = 0.009$), right putamen ($p_{FDR} = 0.019$) with reduced nodal degree observed for the right rolandic operculum ($p_{FDR} = 0.006$) and the left middle temporal pole ($p_{FDR} = 0.007$).

3.1.3. Graph network properties of the DMN

The FDA analysis of network properties of the DMN found no significant differences in path lengths ($p > 0.05$) or normalized clustering ($p > 0.05$) between the two subtypes. Relative to controls, ADHD-C type was found to have significantly shorter characteristic path lengths ($p = 0.01$) but were not different in normalized clustering ($p > 0.05$). No significant differences for DMN properties were observed between ADHD-I type and controls using FDA analysis in path lengths or normalized clustering.

3.2. Voxel-based morphometry analysis

VBM did not yield significant differences between the two subtypes, or relative to controls, for the whole brain or DMN ROI analyses. No volumetric differences were observed in the regions which showed significant differences in nodal degree between the subtypes or comparatively to controls.

4. Discussion

This study examined whether brain structural network organization distinguishes the combined (ADHD-C) and inattentive (ADHD-I) clinical types of ADHD. Graph theoretical analysis revealed altered structural network connectivity pointing to neural differences between the two types. Although global brain network organization did not differ between ADHD-C type and ADHD-I type, we found differential regional network organization in nodal degree. Network properties for the DMN did not significantly differ between the ADHD types from each other. However, a significant shorter characteristic path length was observed in the combined type relative to controls. These network differences were observed in the context of preserved volume between the ADHD-I

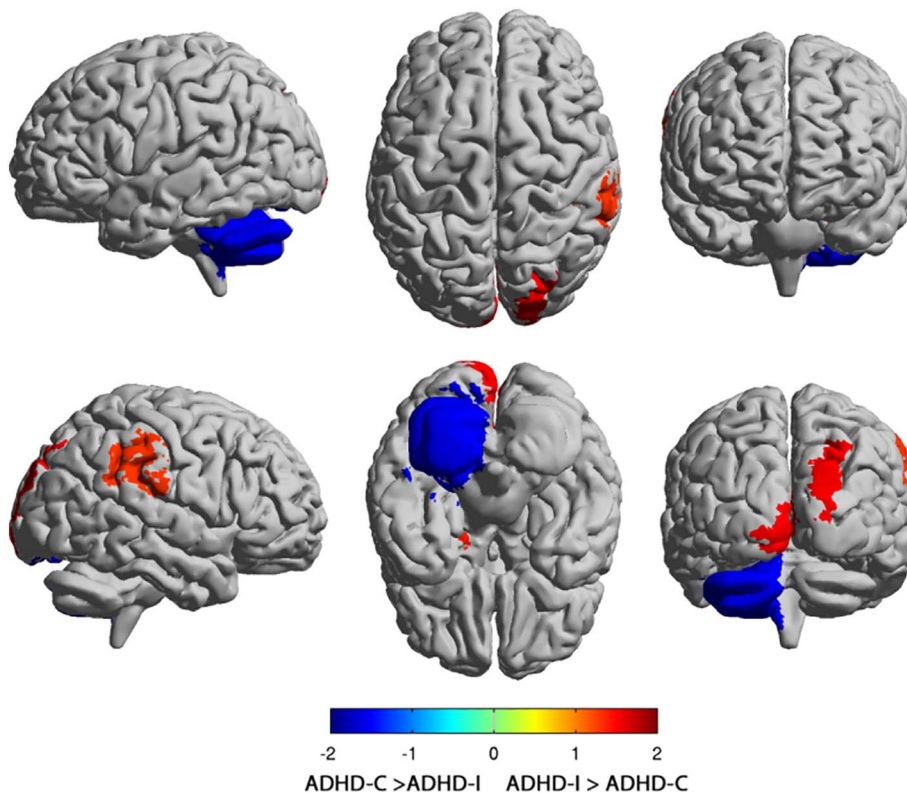


Fig. 2. Group Comparison of regional nodal degree between the Combined (ADHD-C) and Inattentive (ADHD-I) subtypes. Regions with significant group differences in regional degree for networks thresholded at a minimum density of full connectivity overlaid on the ICBM152 surface template. The ADHD-I type exhibited greater nodal degree in the Calcarine (left), Hippocampus (left), the Superior occipital (right), and the Supramarginal gyrus (right). The ADHD-C type exhibited greater nodal degree in the Cerebellum (left). The color bar represents $\log(1/P\text{-value})$. Hot colors indicate regions with higher degree in ADHD-I compared with ADHD-C, while cold colors indicate regions with higher degree in ADHD-C compared with ADHD-I.

and ADHD-C subtypes.

This study used graph theoretical analyses of structural gray matter data in characterizing structural network organization of the combined and inattentive ADHD subtypes. The influence of brain integration and integrative topological properties on the formation of structural covariance networks could represent developmental coordination or synchronized maturation of brain regions. While regions of white matter tracts are shown to be functionally connected (Alexander-Bloch et al., 2013), structural covariance networks also show similar network properties (Irimia & Van Horn, 2013). Interregional structural covariance may perhaps be more characteristic with functional connectivity relative to white matter connections due to the overlap of correlations between brain regions measured by fMRI and gray matter covariance between those regions (Alexander-Bloch et al., 2013).

While there is considerable evidence of altered brain structure in ADHD relative to controls, to our knowledge only three studies that have examined structural volumetric differences between the ADHD-C and ADHD-I subtypes. Our findings are consistent with two out of these studies which also found no significant volumetric differences between the ADHD-C and ADHD-I subtype (Pineda et al., 2002; Vilgis et al., 2016). However, in contrast, one study using a region of interest analysis has reported reduced caudate and ACC volumes in ADHD-C type relative to ADHD-I type and controls (Semrud-Clikeman et al., 2014). Notably, these few studies examining structural differences between the subtypes utilized cohorts comprised of similar clinical composition and sample size. Using the family wise error correction framework in the present study which is typically employed for voxel wise analysis of both structural and functional data, we did not observe volumetric differences between groups. More studies are required to ascertain the volume differences between the ADHD subtypes.

There is now mounting evidence to suggest that global and regional brain networks are altered in ADHD. Using structural covariance measures between regional gray matter volumes in a pooled ADHD sample from the same data sample used in this study, we have previously found greater segregation in global network organization, indexed by significantly increased clustering, relative to controls (Griffiths et al., 2016). Further, ADHD participants have been shown to exhibit less optimized topological organization in their white matter connectome networks (Hirschberger et al., 2007) and decreased global efficiency and increased local efficiency in functional connectome networks comparatively to controls (Nichols & Hayasaka, 2003; Bernhardt et al., 2011). Contrarily, the absence of global network differences in our study for each subtype relative to controls could be due to the limited sample sizes through splitting ADHD participants by subtypes. The lack of global network differences between the two ADHD types could also mean that although overall brain topology properties have been shown to be significantly altered in ADHD, that between the two types, it is largely similar.

However, the analysis of graph network properties of the default mode network (DMN) indicated alterations in ADHD-C type when compared with controls in line with previous functional connectivity results from Fair et al. (Fair et al., 2012a). Path length is a measure of network integration which refers to the efficiency of information exchange and communication along the nodes of a network, therefore shorter path lengths are considered optimal for greater efficiency of communication across the network (Bullmore & Sporns, 2009). Consistent with other studies, findings that continue to show patterns of atypical DMN in ADHD lend support to the view of the DMN as a key network in ADHD pathophysiology (Sripada et al., 2014; Carmona et al., 2005; Fair et al., 2012b). Though no significant subtype differences in DMN properties were found in support of a distinction between ADHD-I and ADHD-C pathophysiology, the ADHD-C type result, relative to controls, is of interest to note. Disruptions to the DMN may explain the characteristic difficulties of attentional and task-goal directed performance in ADHD (Metin et al., 2015). For example, common ADHD behavioral symptoms are often seen in the combined

type involve deficits in attenuated effort or distractibility in task completion, which may be possibly associated with DMN dysregulation (Fassbender et al., 2009).

For the regional network measures, nodal degree differences revealed an interesting pattern between the ADHD-C and ADHD-I subtype with respect to their clinical features. Nodal degree refers to the number of connections that a node has with the rest of the network which biologically has a critical role in understanding the connectivity of that region in terms of its influence on integrative processes and information exchange across the brain (Sporns, 2010). Greater nodal degree implies nodes that are densely distributed, also known as 'hubs', and are considered highly interactive regions of importance relative to functional interactions across the brain network (Sporns, 2013). The ADHD-I type was characterized by greater degree distribution of the regions associated with the limbic, visual and ventral attention networks involving the left hippocampus and the right superior occipital and left calcarine and the right supramarginal gyrus, respectively. On the other hand, in ADHD-C type, higher degree distribution in the cerebellum was found – a region which plays an important role in the motor network and is also known to interact with the frontoparietal executive control circuit. In support of proposed aberrant limbic and frontoparietal network pathways in ADHD (Fair et al., 2012a; Castellanos & Proal, 2012; De La Fuente et al., 2013; Bush, 2011), our network topology results indicate alterations in ADHD-I type in the limbic and parietal attention regions, which are concordant with some of the characteristics of ADHD-I symptoms. The superior occipital and calcarine regions indicated in ADHD-I type are related to the visual network and associated with visual attentional processing deficits that are known to underpin inattentive symptoms in ADHD (Castellanos & Proal, 2012). Specifically, the interplay between the occipital-frontal regions is associated with response inhibition, decision making, emotional control and working memory (Siddiqui et al., 2008), which are all known clinical deficits associated with ADHD-I type. Further, there is evidence that alterations observed in the visual network in ADHD are linked to DMN functioning (Hale et al., 2014) and the ability of the dorsal attention network to maintain and suppress attention to irrelevant stimuli (Castellanos & Proal, 2012). Failing to ignore extraneous stimuli is one of the core symptoms underlying ADHD. The supramarginal gyrus is part of the ventral attention network, and the right supramarginal gyrus has been shown to be involved in attentional shifting (Perry & Zeki, 2000). A disruption of this network is known to underlie distractibility by external stimuli reducing sustained attention to task, with notable difficulties in goal-directed and organizational skills - which are some of the known core symptoms of ADHD-I (Sidlauskaite et al., 2016). Additionally, alterations of the amygdala and hippocampal regions of the limbic system observed in ADHD-I type relative to controls, have been shown to underlie emotion regulation difficulties such as anxiety, social cognition problems, and time management challenges, all of which are characteristic with an ADHD-I symptom profile (Rajmohan & Mohandas, 2007).

Consistent with evidence from structural imaging studies of cerebellar abnormalities in ADHD (Bush, 2010), our network results showed disruptions in the cerebellum in the ADHD-C type. While speculative, this finding could be associated with behavioral difficulties and may extend to excessive physical and verbal activity, restlessness, response inhibition and impulsivity correspondent to ADHD-C features (Castellanos & Proal, 2012). Compared to controls, ADHD-C type also exhibited greater nodal degree in the left anterior cingulum, left middle frontal gyrus and the right putamen with reduced nodal degree in the right rolandic operculum and the left middle temporal gyrus. The anterior cingulum is one of the key nodes of the DMN, and consistent with our DMN analysis results (see above) further lend support to the DMN related alterations that may underpin functional deficits known to the ADHD-C type including impulsivity, disinhibition, distractibility (Diamond, 2005). A greater nodal degree in the putamen, associated

with the salience network (Menon & Toga, 2015), and the middle frontal gyrus a part of the ventral attention network, hold relevance to goal-directed action and attentional processing deficits noted in ADHD. The interactions of these specific networks, specifically with the DMN have been continually proposed to underlie ADHD pathophysiology (Kucyi et al., 2015). However, we note that our study did not directly evaluate correlations of these connectivity measures with cognitive symptoms observed in the two subtypes and hence these associations at this stage are best speculative and should be considered with caution.

Several limitations of this study have been considered in light of our results. Our study is exploratory in nature given the relatively small sample size of this study, which also limits the generalizability of our results. Participant data for hyperactive-impulsive ADHD type was not available and limits a subtype analysis across all three ADHD types in this study. Replication with larger sample sizes is warranted to further explore the possibility of structural abnormalities (Horga et al., 2014). Consistent with previous ADHD research, it is difficult to obtain a “pure” ADHD participant sample, thus there may be confounding effects of medication history and comorbidity (He et al., 2015; Semrud-Clikeman et al., 2006). Larger sample sizes are required to tease out whether structural alterations are confounded with medication history and/or comorbidity. While age and gender were matched in this study, the age range used was 8–17 years. This is a significant period of neurodevelopment and assessing participants using smaller age bands would be useful to address whether these volumetric and network alterations are present, absent or significant at different maturational periods (Nakao et al., 2011). Measures of functional data (fMRI) would contribute to future research to replicate these results from a perspective of functional connectivity patterns in regions associated with the default mode network. The current diagnostic approach of ADHD is limited in its ability to capture the varied presentation of functional impairment among individuals using categorical symptom domains, therefore, diagnostic structures may be better characterized using a framework such as the Research Domain Criteria (RDoC) framework that relies on dimensional constructs. Lastly, while our findings implicate the importance of the brain functional networks associated with symptom profiles of each ADHD subtype, our study did not evaluate the direct correlation of the regional network measures with symptom measures.

5. Conclusion

In summary, we evaluated both volumetric and graph network measures of structural network organization that may characterize the combined and inattentive types of ADHD. We found network alterations in conjunction with preserved volume between the two subtypes and also relative to controls, involving key brain regions that may underpin functional deficits observed in ADHD, and thus may help characterize neurobiological differences between the ADHD Inattentive and ADHD Combined subtype. The emergence of integrated structural and functional network connectivity studies examining connectivity disruption and anatomical network organization, strengthen the ADHD neurobiological framework. Ultimately, insight from imaging research may support the development of brain-based biomarkers to predicate ADHD pathophysiology, improve diagnostic accuracy, treatment prediction and improve clinical outcomes.

Disclosures

Dr. Kohn has received honoraria for educational seminars from Janssen-Cilag, Eli Lilly, and Shire. Dr. Clarke has received honoraria for educational seminars from Eli Lilly and Ciba Geigy. Dr. Griffiths has received honoraria from Shire. Dr. Williams has received research funding from Brain Resource Pty Ltd. for non-salary direct research costs as an investigator on the International Study to Predict Optimized

Treatment in ADHD sites and has previously received consultant fees from Humana. Ms. Saad and Dr. Korgaonkar report no biomedical financial interests or potential conflicts of interest. There are no other conflicts of interest.

Acknowledgements

The iSPOT-A trial was sponsored by Brain Resource Company Operations Pty Ltd. We acknowledge the NHMRC funded Project Grant (APP1008080) awarded to Korgaonkar, Grieve & Williams for the provision of some of the control data. Prof Leanne Williams was the academic Principal Investigator for iSPOT-A (2009–2013), and Prof Simon Clarke was the Principal Investigator for the iSPOT-A Sydney site. Dr. Kristi Griffiths is supported by a Westmead Medical Research Foundation Tenix Foundation Fellowship. Dr. Korgaonkar is supported by an NHMRC Career Development Fellowship (APP1090148). We thank Dr. Lavier Gomes and Ms. Sheryl Foster and the Department of Radiology at Westmead Hospital for their substantial contributions to magnetic resonance imaging data acquisition. We thank Tracey Tsang who served as the iSPOT-A trial coordinator, along with Sariah Hobby, Yennie Hyunh and Jodie Logan who assisted in data acquisition. We also thank the individuals who gave their time to participate in the study.

Appendix A. Supplementary data

Supplementary data to this article can be found online at <http://dx.doi.org/10.1016/j.nicl.2017.05.016>.

References

- Alexander-Bloch, A., Giedd, J.N., Bullmore, E., 2013. Imaging structural co-variance between human brain regions. *Nat. Rev. Neurosci.* 14 (5), 322–336.
- Anderson, A., et al., 2014. Non-negative matrix factorization of multimodal MRI, fMRI and phenotypic data reveals differential changes in default mode subnetworks in ADHD. *NeuroImage* 102 (Pt 1), 207–219.
- Association, A.P., 2013. *Diagnostic and Statistical Manual of Mental Disorders (DSM-5*)*. American Psychiatric Publishing.
- Barber, A.D., et al., 2015. Connectivity supporting attention in children with attention deficit hyperactivity disorder. *NeuroImage* 7, 68–81.
- Batty, M.J., et al., 2010. Cortical gray matter in attention-deficit/hyperactivity disorder: a structural magnetic resonance imaging study. *J. Am. Acad. Child Adolesc. Psychiatry* 49 (3), 229–238.
- Bernhardt, B.C., et al., 2011. Graph-theoretical analysis reveals disrupted small-world organization of cortical thickness correlation networks in temporal lobe epilepsy. *Cereb. Cortex* 21 (9), 2147–2157.
- Bullmore, E., Sporns, O., 2009. Complex brain networks: graph theoretical analysis of structural and functional systems. *Nat. Rev. Neurosci.* 10 (3), 186–198.
- Bush, G., 2010. Attention-deficit/hyperactivity disorder and attention networks. *Neuropsychopharmacology* 35 (1), 278–300.
- Bush, G., 2011. Cingulate, frontal and parietal cortical dysfunction in attention-deficit/hyperactivity disorder. *Biol. Psychiatry* 69 (12), 1160–1167.
- Cao, M., et al., 2014. Imaging functional and structural brain connectomics in attention-deficit/hyperactivity disorder. *Mol. Neurobiol.* 50 (3), 1111–1123.
- Carmona, S., et al., 2005. Global and regional gray matter reductions in ADHD: a voxel-based morphometric study. *Neurosci. Lett.* 389 (2), 88–93.
- Carmona, S., et al., 2015. Sensation-to-cognition cortical streams in attention-deficit/hyperactivity disorder. *Hum. Brain Mapp.* 36 (7), 2544–2557.
- Castellanos, F.X., Proal, E., 2012. Large-scale brain systems in ADHD: beyond the prefrontal-striatal model. *Trends Cogn. Sci.* 16 (1), 17–26.
- Cortese, S., et al., 2012. Toward systems neuroscience of ADHD: a meta-analysis of 55 fMRI studies. *Am. J. Psychiatr.* 169 (10), 1038–1055.
- De La Fuente, A., et al., 2013. A review of attention-deficit/hyperactivity disorder from the perspective of brain networks. *Front. Hum. Neurosci.* 7, 192.
- Dey, S., Rao, A.R., Shah, M., 2012. Exploiting the brain's network structure in identifying ADHD subjects. *Front. Syst. Neurosci.* 6, 75.
- Diamond, A., 2005. Attention-deficit disorder (attention-deficit/hyperactivity disorder without hyperactivity): a neurobiologically and behaviorally distinct disorder from attention-deficit/hyperactivity disorder (with hyperactivity). *Dev. Psychopathol.* 17 (3), 807–825.
- DuPaul, G.J., 1998. *ADHD Rating Scale-IV: Checklists, Norms, and Clinical Interpretation*. Guilford Press.
- Elliott, G.R., et al., 2014. Cognitive testing to identify children with ADHD who do and do not respond to methylphenidate. *J. Atten. Disord.*
- Ercan, E.S., et al., 2016. Altered structural connectivity is related to attention deficit/hyperactivity subtypes: a DTI study. *Psychiatry Res. Neuroimaging.* 256, 57–64.

- Fair, D.A., et al., 2008. The maturing architecture of the brain's default network. *Proc. Natl. Acad. Sci. U. S. A.* 105 (10), 4028–4032.
- Fair, D.A., et al., 2010. Atypical default network connectivity in youth with attention-deficit/hyperactivity disorder. *Biol. Psychiatry* 68 (12), 1084–1091.
- Fair, D.A., et al., 2012a. Distinct neural signatures detected for ADHD subtypes after controlling for micro-movements in resting state functional connectivity MRI data. *Front. Syst. Neurosci.* 6, 80.
- Fair, D.A., et al., 2012b. Distinct neuropsychological subgroups in typically developing youth inform heterogeneity in children with ADHD. *Proc. Natl. Acad. Sci. U. S. A.* 109 (17), 6769–6774.
- Faraone, S.V., et al., 2015. Attention-deficit/hyperactivity disorder. In: *Nature Reviews Disease Primers*. Macmillan Publishers Limited, pp. 15020.
- Fassbender, C., et al., 2009. A lack of default network suppression is linked to increased distractibility in ADHD. *Brain Res.* 1273, 114–128.
- Griffiths, K.R., Grieve, S.M., Kohn, M.R., Clarke, S., Williams, L.M., Korgaonkar, M.S., 2016. Altered gray matter organization in children and adolescents with ADHD: a structural covariance connectome study. *Transl. Psychiatry*.
- Hale, T.S., et al., 2014. Visual network asymmetry and default mode network function in ADHD: an fMRI study. *Front. Psych.* 5, 81.
- He, Y., Evans, A., 2010. Graph theoretical modeling of brain connectivity. *Curr. Opin. Neurol.* 23 (4), 341–350.
- He, Y., Chen, Z.J., Evans, A.C., 2007. Small-world anatomical networks in the human brain revealed by cortical thickness from MRI. *Cereb. Cortex* 17 (10), 2407–2419.
- He, N., et al., 2015. Neuroanatomical deficits correlate with executive dysfunction in boys with attention deficit hyperactivity disorder. *Neurosci. Lett.* 600, 45–949.
- Hirschberger, M., Qi, Y., Steuer, R.E., 2007. Randomly generating portfolio-selection covariance matrices with specified distributional characteristics. *Eur. J. Oper. Res.* 177 (3), 1610–1625.
- Hong, S.B., et al., 2014. Connectomic disturbances in attention-deficit/hyperactivity disorder: a whole-brain tractography analysis. *Biol. Psychiatry* 76 (8), 656–663.
- Horga, G., Kaur, T., Peterson, B.S., 2014. Annual research review: current limitations and future directions in MRI studies of child- and adult-onset developmental psychopathologies. *J. Child Psychol. Psychiatry* 55 (6), 659–680.
- Hosseini, S.M., Hoefl, F., Kesler, S.R., 2012. GAT: a graph-theoretical analysis toolbox for analyzing between-group differences in large-scale structural and functional brain networks. *PLoS One* 7 (7), e40709.
- Iannaccone, R., et al., 2015. Classifying adolescent attention-deficit/hyperactivity disorder (ADHD) based on functional and structural imaging. *Eur. Child Adolesc. Psychiatry* 24 (10), 1279–1289.
- Irimia, A., Van Horn, J.D., 2013. The structural, connectomic and network covariance of the human brain. *NeuroImage* 0, 489–499.
- Kucy, A., et al., 2015. Disrupted functional connectivity of cerebellar default network areas in attention-deficit/hyperactivity disorder. *Hum. Brain Mapp.* 36 (9), 3373–3386.
- Lee, S.S., Sibley, M.H., Epstein, J.N., 2016. Attention-deficit/hyperactivity disorder across development: predictors, resilience, and future directions. *J. Abnorm. Psychol.* 125 (2), 151–153.
- Lei, D., et al., 2014a. Microstructural abnormalities in the combined and inattentive subtypes of attention deficit hyperactivity disorder: a diffusion tensor imaging study. *Sci. Rep.* 4.
- Lei, D., et al., 2014b. Microstructural abnormalities in the combined and inattentive subtypes of attention deficit hyperactivity disorder: a diffusion tensor imaging study. *Sci. Rep.* 4, 6875.
- Liddle, E.B., et al., 2011. Task-related default mode network modulation and inhibitory control in ADHD: effects of motivation and methylphenidate. *J. Child Psychol. Psychiatry* 52 (7), 761–771.
- Lin, H.Y., et al., 2015. Altered resting-state frontoparietal control network in children with attention-deficit/hyperactivity disorder. *J. Int. Neuropsychol. Soc.* 21 (4), 271–284.
- Maldjian, J.A., et al., 2003. An automated method for neuroanatomic and cytoarchitectonic atlas-based interrogation of fMRI data sets. *NeuroImage* 19 (3), 1233–1239.
- de Mello, C.B., et al., 2013. Neuroimaging and neuropsychological analyses in a sample of children with ADHD-inattentive subtype. *Clin. Neuropsychiatry* 10 (2).
- Menon, V., Toga, A., 2015. *Brain Mapping: An Encyclopedic Reference*.
- Metin, B., et al., 2015. Dysfunctional modulation of default mode network activity in attention-deficit/hyperactivity disorder. *J. Abnorm. Psychol.* 124 (1), 208–214.
- Mohan, A., et al., 2016. The significance of the default mode network (DMN) in neurological and neuropsychiatric disorders: a review. *Yale J. Biol. Med.* 89 (1), 49–57.
- Nakao, T., et al., 2011. Gray matter volume abnormalities in ADHD: voxel-based meta-analysis exploring the effects of age and stimulant medication. *Am. J. Psychiatry* 168 (11), 1154–1163.
- Nichols, T., Hayasaka, S., 2003. Controlling the familywise error rate in functional neuroimaging: a comparative review. *Stat. Methods Med. Res.* 12 (5), 419–446.
- Orinstein, A.J., Stevens, M.C., 2014. Brain activity in predominantly-inattentive subtype attention-deficit/hyperactivity disorder during an auditory oddball attention task. *Psychiatry Res. Neuroimaging* 223 (2), 121–128.
- Park, B.Y., et al., 2016. Connectivity analysis and feature classification in attention deficit hyperactivity disorder sub-types: a task functional magnetic resonance imaging study. *Brain Topogr.* 29 (3), 429–439.
- Perry, R.J., Zeki, S., 2000. The neurology of saccades and covert shifts in spatial attention: an event-related fMRI study. *Brain* 123 (Pt 11), 2273–2288.
- Peterson, B.S., et al., 2009. An fMRI study of the effects of psychostimulants on default-mode processing during Stroop task performance in youths with ADHD. *Am. J. Psychiatry* 166 (11), 1286–1294.
- Pineda, D.A., et al., 2002. Statistical analyses of structural magnetic resonance imaging of the head of the caudate nucleus in Colombian children with attention-deficit hyperactivity disorder. *J. Child Neurol.* 17 (2), 97–105.
- Posner, J., Park, C., Wang, Z., 2014. Connecting the dots: a review of resting connectivity MRI studies in attention-deficit/hyperactivity disorder. *Neuropsychol. Rev.* 24 (1), 3–15.
- Qiu, M.G., et al., 2011. Changes of brain structure and function in ADHD children. *Brain Topogr.* 24 (3–4), 243–252.
- Raichle, M.E., 2015. The brain's default mode network. *Annu. Rev. Neurosci.* 38, 433–447.
- Rajmohan, V., Mohandas, E., 2007. The limbic system. *Indian J. Psychiatry* 49 (2), 132–139.
- Rubinov, M., Sporns, O., 2010. Complex network measures of brain connectivity: uses and interpretations. *NeuroImage* 52 (3), 1059–1069.
- Saad, J.F., et al., 2015. Is the theta/beta EEG marker for ADHD inherently flawed? *J. Atten. Disord.*
- dos Santos Siqueira, A., et al., 2014. Abnormal functional resting-state networks in ADHD: graph theory and pattern recognition analysis of fMRI data. *Biomed. Res. Int.* 2014, 380531.
- Seidman, L.J., Valera, E.M., Makris, N., 2005. Structural brain imaging of attention-deficit/hyperactivity disorder. *Biol. Psychiatry* 57 (11), 1263–1272.
- Semrud-Clikeman, M., et al., 2006. Volumetric MRI differences in treatment-naive vs chronically treated children with ADHD. *Neurology* 67 (6), 1023–1027.
- Semrud-Clikeman, M., et al., 2014. Regional volumetric differences based on structural MRI in children with two subtypes of ADHD and controls. *J. Atten. Disord.*
- Shaw, P., et al., 2007. Attention-deficit/hyperactivity disorder is characterized by a delay in cortical maturation. *Proc. Natl. Acad. Sci. U. S. A.* 104 (49), 19649–19654.
- Sheehan, D.V., et al., 1998. The Mini-International Neuropsychiatric Interview (MINI): the development and validation of a structured diagnostic psychiatric interview for DSM-IV and ICD-10. *J. Clin. Psychiatry*.
- Siddiqui, S.V., et al., 2008. Neuropsychology of prefrontal cortex. *Indian J. Psychiatry* 50 (3), 202–208.
- Sidlauskaitė, J., et al., 2016. Altered intrinsic organisation of brain networks implicated in attentional processes in adult attention-deficit/hyperactivity disorder: a resting-state study of attention, default mode and salience network connectivity. *Eur. Arch. Psychiatry Clin. Neurosci.* 266 (4), 349–357.
- Silk, T., et al., 2005. Fronto-parietal activation in attention-deficit hyperactivity disorder, combined type: functional magnetic resonance imaging study. *Br. J. Psychiatry* 187, 282–283.
- Singh, M.K., et al., 2013. Anomalous gray matter structural networks in major depressive disorder. *Biol. Psychiatry* 74 (10), 777–785.
- Solanto, M.V., et al., 2009. Event-related fMRI of inhibitory control in the predominantly inattentive and combined subtypes of ADHD. *J. Neuroimaging* 19 (3), 205–212.
- Sporns, O., 2010. *Networks of the Brain*. MIT Press.
- Sporns, O., 2013. Structure and function of complex brain networks. *Dialogues Clin. Neurosci.* 15 (3), 247–262.
- Sripada, C., et al., 2014. Disrupted network architecture of the resting brain in attention-deficit/hyperactivity disorder. *Hum. Brain Mapp.* 35 (9), 4693–4705.
- Stevens, M.C., Pearson, G.D., Kiehl, K.A., 2007. An fMRI auditory oddball study of combined-subtype attention deficit hyperactivity disorder. *Am. J. Psychiatry* 164 (11), 1737–1749.
- Svatkova, A., et al., 2016. Unique white matter microstructural patterns in ADHD presentations—a diffusion tensor imaging study. *Hum. Brain Mapp.* (pp. n/a-n/a).
- Tomasi, D., Volkow, N.D., 2012. Abnormal functional connectivity in children with attention-deficit/hyperactivity disorder. *Biol. Psychiatry* 71 (5), 443–450.
- Valera, E.M., et al., 2007. Meta-analysis of structural imaging findings in attention-deficit/hyperactivity disorder. *Biol. Psychiatry* 61.
- Vilgis, V., et al., 2016. Global and local grey matter reductions in boys with ADHD combined type and ADHD inattentive type. *Psychiatry Res.* 254, 119–126.
- Wang, X.H., Li, L., 2015. Altered temporal features of intrinsic connectivity networks in boys with combined type of attention deficit hyperactivity disorder. *Eur. J. Radiol.* 84 (5), 947–954.
- Weissman, D.H., et al., 2006. The neural bases of momentary lapses in attention. *Nat. Neurosci.* 9 (7), 971–978.
- Wellington, T.M., et al., 2006. Magnetic resonance imaging volumetric analysis of the putamen in children with ADHD: combined type versus control. *J. Atten. Disord.* 10 (2), 171–180.
- Wilke, M., et al., 2008. Template-O-Matic: a toolbox for creating customized pediatric templates. *NeuroImage* 41 (3), 903–913.
- Willcutt, E.G., 2012. The prevalence of DSM-IV attention-deficit/hyperactivity disorder: a meta-analytic review. *Neurotherapeutics* 9 (3), 490–499.